Supporting Information

Wakano et al. 10.1073/pnas.0812644106

SI Text

Model Analysis. Consider the following selection–diffusion dynamics for the density of cooperators, $u(x, y, t)$, and defectors, $v(x, y, t)$, as a function of the spatial coordinates x, y, and time t:

$$\partial_t u = D_C \nabla^2 u + u[w(f_C + b) - d] \quad \text{[S1a]}$$

$$\partial_t v = D_D \nabla^2 v + v[w(f_D + b) - d] \quad \text{[S1b]}$$

The per capita birth rate of cooperators and defectors, $w(f_C + b)$ and $w(f_D + b)$, is determined by the baseline birthrate, b, their performance in public-goods interactions, f_C and f_D, respectively, and is negatively correlated with the population density $u + v$ through $w = 1 - u - v$. Thus, competition results in decreasing birth rates for increasing population densities and vice versa. The per capita death rate, d, is equal and constant for both types. Spatial migration of cooperators and defectors is determined by the diffusion constants, D_C and D_D, and the diffusion operator $\nabla^2 = \partial_x^2 + \partial_y^2$, where ∂_i denotes the shorthand notation for the partial derivative with respect to i. The spatial domain Ω is $L \times L$, where L denotes the linear extension of space, unless otherwise specified. We only consider Neumann boundary condition (i.e., zero-flux boundaries).

Derivation of payoffs. Public-goods games are played in randomly formed groups with a maximum size of N. Participants are sampled by interpreting the densities u (v) as probabilities for drawing a cooperator (defector) and w for failing to find a participant, respectively. Thus, the population density, $u + v$, determines the effective interaction group size S with an average size of $(u + v)N$. An individual finds itself in a group of size S with probability

$$\binom{N-1}{S-1}(1-w)^{S-1}w^{N-S}.$$

In this group, the individual faces m cooperators and $S - 1 - m$ defectors with probability

$$\binom{S-1}{m}\left(\frac{u}{u+v}\right)^m\left(\frac{v}{u+v}\right)^{S-1-m}$$

and the payoff for defectors and cooperators is given by

$$P_D(S) = \frac{r}{S}\sum_{m=0}^{S-1}\binom{S-1}{m}m\left(\frac{u}{u+v}\right)^m\left(\frac{v}{u+v}\right)^{S-1-m} \quad \text{[S2a]}$$

$$P_C(S) = P_D(S) + \frac{r}{S} - 1. \quad \text{[S2b]}$$

For convenience, the costs of cooperation are set to $c = 1$. Averaging over all group sizes S yields

$$f_i = \sum_{S=2}^{N}\binom{N-1}{S-1}(1-w)^{S-1}w^{N-S}P_i(S)$$

with $i = C$ or D and reduces to

$$f_D = r\frac{u}{1-w}\left(1 - \frac{1-w^N}{N(1-w)}\right) \quad \text{[S3a]}$$

$$f_C = f_D - F(w) \quad \text{[S3b]}$$

$$F(w) = 1 + (r-1)w^{N-1} - \frac{r}{N}\frac{1-w^N}{1-w}. \quad \text{[S3c]}$$

The difference between the payoffs of cooperators and defectors, $F(w)$, is always positive for $r < 2$ such that defectors prevail. For $r > 2$, $F(w) = 0$ has a single and unique root $\hat{w} \in [0,1)$ (1). For $w > \hat{w}$, $F(w) < 0$ holds, and hence, cooperators thrive. A more detailed derivation and analysis is provided in refs. 2 and 3).

Nonspatial dynamics. The dynamics in the absence of space (see Eq. **1** in the main text), which corresponds to Eq. **S1** without the diffusion terms $D_C\nabla^2 u$ and $D_D\nabla^2 v$) reduces to a set of ordinary differential equations (ODE) that can be analyzed in detail (3). This provides the basis for the analysis of the spatial system of partial differential equations (PDE) in Eq. **S1**. Here, we focus on the scenario with baseline birthrates $b \geq 1$ and the more interesting case with death rates $d < b$, such that defectors cannot survive in the absence of cooperators ($\partial_t v < 0$ for $u = 0$). In this case, the ODE admits 2 fixed points that are of particular interest: **O** and **Q**. The state **O** denotes the extinction of the population ($u = 0, v = 0$) and is always stable. The existence and stability of **Q**, where cooperators and defectors can coexist, depends on the multiplication factor of the public good, r, but the thresholds of r are analytically inaccessible because $\hat{w}$ cannot be determined for arbitrary N. However, it can be shown that **Q** is unique, if it exists (3). A lower bound for the existence of **Q** is given by $r > 2$ because otherwise $\hat{w}$ does not exist. At r_{Hopf}, the system undergoes a subcritical Hopf bifurcation (4) that gives rise to unstable limit cycles for r close to but above r_{Hopf}. Note that with $b \geq 1$, supercritical Hopf bifurcations accompanied by stable limit cycles are impossible (3). For $r < r_{\text{Hopf}} = 2.3658$, **Q** is unstable and **O** is globally stable (numerical values are provided for the parameters used in all figures, $N = 8$, $b = 1$, $d = 1.2$). For $r_{\text{Hopf}} < r < r_2 = 6.53$, **Q** is stable, and the basin of attraction increases with r but remains limited. For unfavorable initial configurations, either because of low population densities that result in a shortage of interaction partners [as described by the Allee effect (5)] or because of high relative abundance of defectors that diminish the public good, the population cannot recover and goes extinct, i.e., converges to **O**. Finally, for high multiplication factors, $r > r_2$, defectors disappear and cooperators thrive unchallenged.

Spatial Dynamics

Selection and diffusion in spatial ecological public-goods games can trigger spontaneous pattern formation through diffusion-induced instability (Turing instability) or diffusion-induced coexistence. The heterogeneous density distributions of cooperators and defectors can be static, quasistatic with intermittent bursts of rapid changes or dynamic patterns of spatiotemporal chaos. The different dynamical regimes are summarized in a schematic phase plane diagram, Fig. S1.

Diffusion-Induced Instability. If the coexistence equilibrium **Q** exists and is stable in the absence of spatial extension ($r > r_{\text{Hopf}}$), then diffusion can destabilize **Q** because the ecological public-goods game represents an activator–inhibitor system (6, 7) in the vicinity of **Q**. The Jacobian matrix **J** at **Q** is given by

$$J = \begin{pmatrix} J_{11} & J_{21} \\ J_{12} & J_{22} \end{pmatrix} = \begin{pmatrix} -u\frac{d}{w} + uw\partial_u f_C & -u\frac{d}{w} + uw\partial_v f_C \\ -v\frac{d}{w} + vw\partial_u f_D & -v\frac{d}{w} + vw\partial_v f_D \end{pmatrix}. \quad \text{[S4]}$$

The fitness of cooperators and defectors is determined by their performance in public-goods interactions and adjusted by the population density. Increasing population densities (and hence decreasing w) reduces the fitness, which is reflected in the negative first term in each component of **J**. The second term indicates the effect of population densities on the payoffs. It is easy to see that increasing the defector density reduces the payoffs of both cooperators and defectors, i.e., $\partial_v f_C < 0$ and $\partial_v f_D < 0$ (see Eq. **S3**. Thus, defectors act as inhibitors. Similarly, increasing the cooperator density increases the payoffs of both types, i.e., $\partial_u f_C > 0$ and $\partial_u f_D > 0$, which indicates that cooperators act as activators whenever the population densities are sufficiently low. An activator–inhibitor system requires $J_{1i} > 0$ and $J_{2i} < 0$ at **Q**.

In this case, diffusion induced instability (or Turing instability) occurs if inhibitors (defectors) diffuse faster than activators (cooperators). Various critical parameters can be calculated that determine the spatial pattern formation (6–8). In particular, we can derive the minimum ratio of the diffusion coefficients of inhibitors and activators, D_D/D_C, as well as the characteristic length scale, l, of the emerging patterns (see *Pattern formation process* below). Any spatial perturbation in the square domain Ω is decomposed into spatial modes

$$\cos\frac{n\pi x}{L}\cos\frac{m\pi y}{L}. \qquad \text{[S5]}$$

with spatial eigenvalues $k^2 = \pi^2(n^2 + m^2)/L^2$, where n,m are integers. The linearlized temporal dynamics of each spatial mode is given by

$$\frac{d}{dt}\begin{pmatrix} u_k \\ v_k \end{pmatrix} = \left[\mathrm{J} - k^2 \begin{pmatrix} D_C & 0 \\ 0 & D_D \end{pmatrix} \right] \begin{pmatrix} u_k \\ v_k \end{pmatrix}, \qquad \text{[S6]}$$

where $\begin{pmatrix} u_k \\ v_k \end{pmatrix}$ denotes deviations from **Q**. The dynamics is not necessarily stable even if it is stable against homogeneous perturbations (i.e., $n = m = 0$ or $k = 0$). The necessary and sufficient condition for instability is determined by **J**, D_C, D_D and k. In particular, if we neglect the condition that n,m should be integers, the minimum ratio of diffusion coefficient is given by

$$\frac{D_D}{D_C} > \frac{-2J_{21}+J_{12}+J_{11}J_{22}+2\sqrt{-J_{12}J_{21}\det \mathrm{J}}}{J_{11}^2}. \qquad \text{[S7]}$$

The minimum ratio must be >1. Numerically we obtain J_{ij} to confirm that the system satisfies the conditions for activator–inhibitor dynamics and derive the threshold value for D_D/D_C that is required for the spontaneous emergence of spatial patterns (see Fig. S1).

Pattern formation process. The pattern formation process can be understood and analyzed in greater detail in a 1-dimensional spatial setting. The most unstable mode, k^*, (with the largest eigenvalue λ_{k^*}) determines the characteristic length scale, l, of the emerging patterns with $l = 2\pi/k^*$. k^* is estimated by $d\lambda_k/dk = 0$ where

$$\lambda_k = \frac{1}{2}\left(J_{11} + J_{22} - k^2(D_C + D_D) + \sqrt{\begin{array}{l}(J_{11} + J_{22} - k^2(D_C + D_D))^2 \\ -4(\det \mathrm{J} - k^2(D_C J_{22} + D_D J_{11}) + k^4 D_C D_D)\end{array}}\right). \qquad \text{[S8]}$$

The analytic estimation of l provides an excellent approximation of the characteristic scale for the observed patterns both in 1 dimension (see Fig. S2) and in 2-dimensional space (see Fig. 2*A* in the main text).

Starting from an initially homogeneous distribution with densities near **Q** and a small disturbance in the center, then the spreading of the disturbance nicely illustrates the pattern formation process (see Fig. S2). First the perturbation grows, and the densities of cooperators and defectors increases. Due to the higher diffusion rate of defectors, cooperators suffer in the adjacent regions on either side, which decreases the densities of both strategies. The low defector densities then enable cooperators still further away from the initial perturbation to thrive, which triggers an increase in both strategies. This process repeats until the boundaries are reached. The distance between subsequent density peaks (or valleys) depends on the diffusion coefficients, D_C, D_D, and indicates the characteristic length scale, l.

Diffusion-induced coexistence. Diffusion-induced coexistence is closely related to diffusion-induced instability with the only difference being that the coexistence equilibrium **Q** is unstable in the absence of space ($r < r_{\mathrm{Hopf}}$). Consequently, any deviation from **Q** is amplified over time in an oscillatory manner until the population goes extinct and reaches the globally stable equilibrium **O**. In the vicinity of $r = r_{\mathrm{Hopf}}$, the system again exhibits an activator–inhibitor dynamics, and the analysis of the Jacobian **J** at **Q** remains the same. Indeed, cooperators behave as activators as long as $r < r_{\mathrm{Turing}} = 3.31$. However, the homogeneous mode ($k = 0$) is already unstable, and a linear analysis is less powerful for diffusion-induced instability. Only recently, diffusion-induced coexistence attracted increasing attention (9), but a rigorous analysis is lacking. Diffusion-induced coexistence is not restricted to static patterns but allows much richer dynamics, which include spatiotemporal chaos (see Fig. S1).

The detailed pattern formation process for diffusion-induced coexistence is again nicely illustrated when considering a 1-dimensional system with a homogeneous initial distribution with densities of cooperators and defectors near **Q** and a small disturbance in the center. The densities in homogeneous regions oscillate and approach extinction, **O**, but the disturbance spreads and establishes stable heterogeneous strategy distributions (see Fig. S3). The basic spreading of the disturbance is the same as for diffusion-induced instability (see Fig. S2), because in both cases, the propagation is driven by the activator-inhibitor dynamics. In addition, the instability of **Q** manifests itself near the front of the propagating disturbance in that defectors destabilize peaks of high cooperator densities and repeatedly split them into 2 peaks until the boundaries are reached, and a stable heterogeneous strategy distribution takes shape.

Robustness of Results. To support our claims that spatial pattern formation promotes cooperation, we verified the robustness of our results for different initial configurations as well as other numerical methods and domain shapes.

Numerics. For the numerical integration of Eq. **S1**, the spatial domain is discretized by a square grid with an equal spacing of dx in both dimensions, and the time evolution is determined by using the Crank–Nicholson method (10) in time increments dt. Results in the chaotic regime are particularly sensitive to numerical methods. To verify the robustness, the numerical integration shown in Fig. 1 of the main text was carried out for all combinations of $dx = 0.25, 0.4, 1.0, 2, 4$ and $dt = 0.001, 0.01, 0.1, 1$. No qualitative differences were found for any combination. In addition, we checked the results using a different method based on finite elements [Hecht F, Pironneau O, Le Hyaric A, Ohtsuka K (2007) Freefem++: Finite element method to solve partial differential equations. www.freefem.org] with different boundary shapes (see Fig. 4). Again, no qualitative differences were found.

Initial configuration. Numerical integration of PDEs is often susceptible to changes in the initial configuration. To verify the robustness of the pattern formation, we carried out simulations using initial configurations with a homogeneous disk of equal densities of cooperators and defectors located in the center of vacant space (see Fig. S5) instead of heterogeneous distributions

of random cooperator and defector densities (see Fig. 4 in main text). The qualitative features of the dynamics and the characteristic patterns remain unchanged. Only the boundaries of the chaotic regime are slightly different, but this is not surprising because this regime is defined by its susceptibility with respect to small configurational changes.

Patterns. In the absence of space, the basin of attraction of the coexistence equilibrium **Q** is determined by r. For $r \leq r_{\mathrm{Hopf}}$, **Q** is unstable, and the population invariably disappears (the extinction state **O** with $w = 1$ is globally stable). For $r > r_{\mathrm{Hopf}}$, **Q** is stable, and the basin of attraction increases with r, but **O** remains locally stable for any r. The dynamics of the nonspatial ODE is shown in Fig. S6*a*. Spatial extension and diffusion enlarge the basin of attraction of **Q** by forming heterogeneous strategy distributions. Because measuring the basin of attraction is challenging, we consider r just below r_{Hopf} such that **O** is globally stable in the absence of space. Nevertheless, in the spatial system, cooperators and defectors coexist (see Fig. S6*b*) for a broad range of initial population densities. Thus, spatial extension sustains the population by maintaining cooperation through pattern formation.

1. Hauert C, De Monte S, Hofbauer J, Sigmund K (2002) Replicator dynamics in optional public goods games. *J Theor Biol* 218:187–194.
2. Hauert C, Holmes M, Doebeli M (2006) Evolutionary games and population dynamics: maintenance of cooperation in public goods games. *Proc R Soc London Ser B* 273:2565–2570.
3. Hauert C, Wakano JY, Doebeli M (2008) Ecological public goods games: cooperation and bifurcation. *Theor Pop Biol* 73:257–263.
4. Kuznetsov YA (2004) *Elements of Applied Bifurcation Theory* (Springer, New York).
5. Stephens PA, Sutherland WJ (1999) Consequences of the Allee effect for behavior, ecology and conservation. *Trends Ecol Evol* 14:401–405.
6. Murray J (2003) *Mathematical Biology II: Spatial Models and Biomedial Applications* (Springer, Berlin).
7. Segel LA, Jackson JL (1972) Dissipative structure: An explanation and an ecological example. *J Theor Biol* 37:545–559.
8. Turing AM (1952) The chemical basis of morphogenesis. *Phil Trans R Soc London Ser B* 237:37–72.
9. Baurmann M, Gross T, Feudel U (2007) Instabilities in spatially extended predator–prey systems: Spatio-temporal patterns in the neighborhood of Turing–Hopf bifurcations. *J Theor Biol* 245:220–229.
10. Press WH, Teukolsky SA, Vetterling WT, Flannery BP (1988) *Numerical Recipes in C* (Cambridge Univ Press, Cambridge, UK).

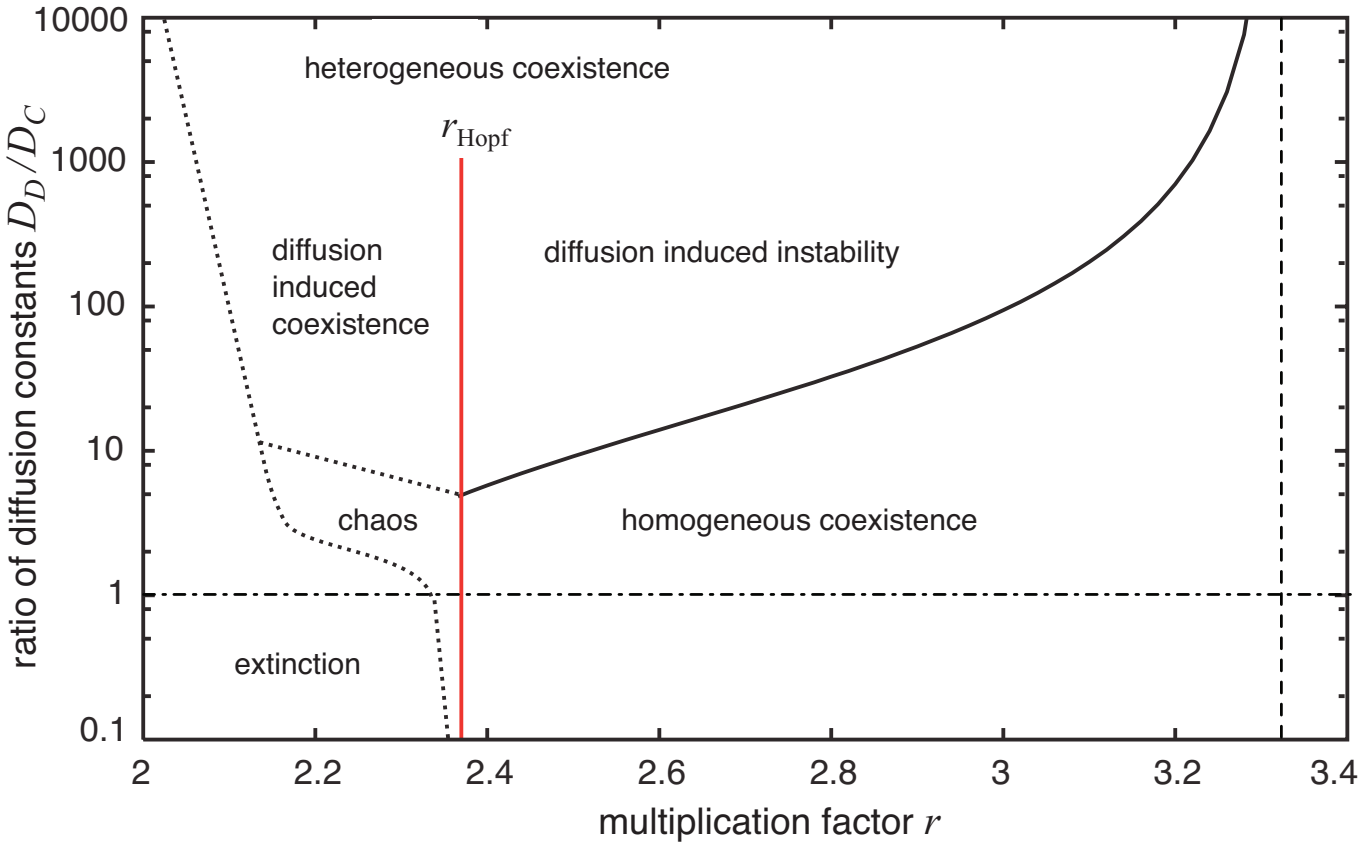

Fig. S1. Schematic phase plane diagram of the different dynamical regimes in terms of the ratio of the diffusion of defectors to cooperators, D_D/D_C and the multiplication factor r in spatial ecological public goods games. The vertical red line indicates r_{Hopf}, which separates the region of extinction ($r < r_{\mathrm{Hopf}}$) and possible stable coexistence ($r > r_{\mathrm{Hopf}}$) in the absence of space. If cooperator diffusion exceeds defector diffusion, $D_D/D_C < 1$ the dynamics is barely affected by space, except for a small chaotic region near r_{Hopf}. The dashed lines indicate approximate boundaries based on numerical results. These thresholds are analytically inaccessible and for the chaotic region even numerically challenging because the sensitivity of the system with respect to initial configurations increases when approaching the boundary of the parameter range where the population persists. The dynamics becomes much richer for $D_D/D_C > 1$. For $r < r_{\mathrm{Hopf}}$, the chaotic regime increases substantially and is replaced by diffusion-induced coexistence for high D_D/D_C. For $r > r_{\mathrm{Hopf}}$ the homogeneous spatial distributions are replaced by heterogeneous distributions triggered by diffusion induced instability (Turing patterns) for high D_D/D_C. The solid line indicates the analytical threshold ratio of the diffusion constants required for Turing patterns (see Eq. **S7**.) For very large $r > r_{\mathrm{Turing}} = 3.32$ (shown by the vertical dashed line) all patterns disappear. All thresholds refer to $N = 8$, $d = 1.2$, $b = 1$, $D_C = 1$ and are based on numerical integration using $L = 283$, $dx = 1.4$, $dt = 0.1$.

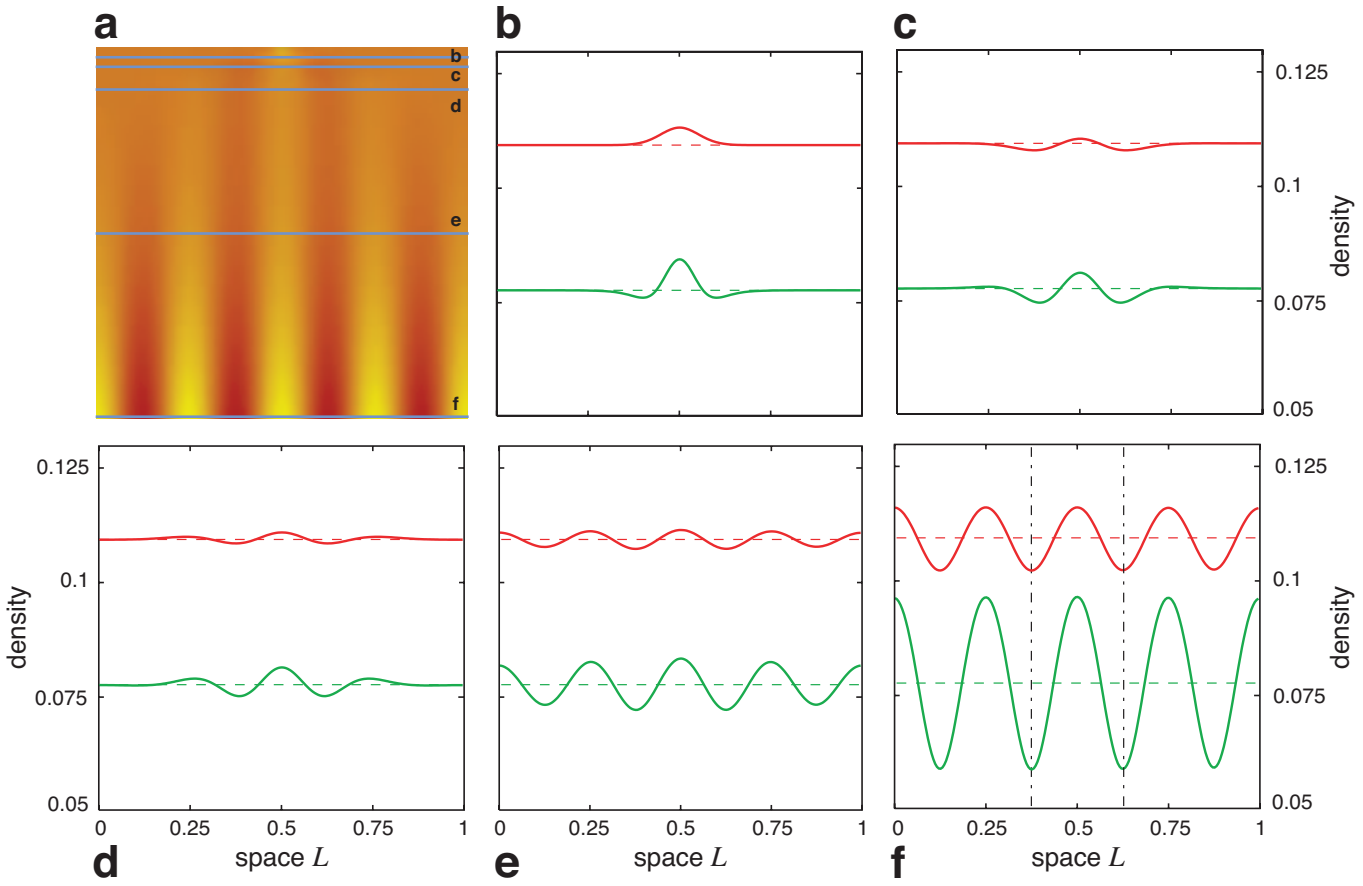

Fig. S2. Pattern formation process in ecological public goods games through diffusion-induced instability in 1-dimensional spatial systems. Initially the strategy distribution is homogeneous with densities near the stable coexistence equilibrium **Q** and a perturbation in the center (increase of the cooperator density by 0.1). (*a*) Space–time plot of the pattern formation process where the abscissa denotes space, and the ordinate the time (from top to bottom). The brightness of the colors indicates the density of cooperators (green) and defectors (red) or both (yellow). The horizontal lines in *a*, labeled b–f, indicate the times of the cross-sections of cooperator (green) and defector (red) densities in $t = 10$ (*b*), $t = 24$ (*c*), t = 40 (*d*), $t = 200$ (*e*), and $t = 398$ (*f*). In *b*–*f*, the dashed horizontal lines indicate the equilibrium frequencies of cooperators, $\hat{u}$, and defectors, $\hat{v}$ at **Q**. The dashed vertical lines in *f* indicate the characteristic length scale, *l*, according to Eq. **S8**. The game parameters are $N = 8$, $b = 1$, $d = 1.2$, $r = 2.5$, which yield $\hat{u} = 0.078$ and $\hat{v} = 0.11$. Diffusion coefficients are $D_C = 1$ and $D_D = 10$, spatial extension is $L = 100$ and numerical integration uses $dx = 0.5$ and time increments of $dt = 0.1$.

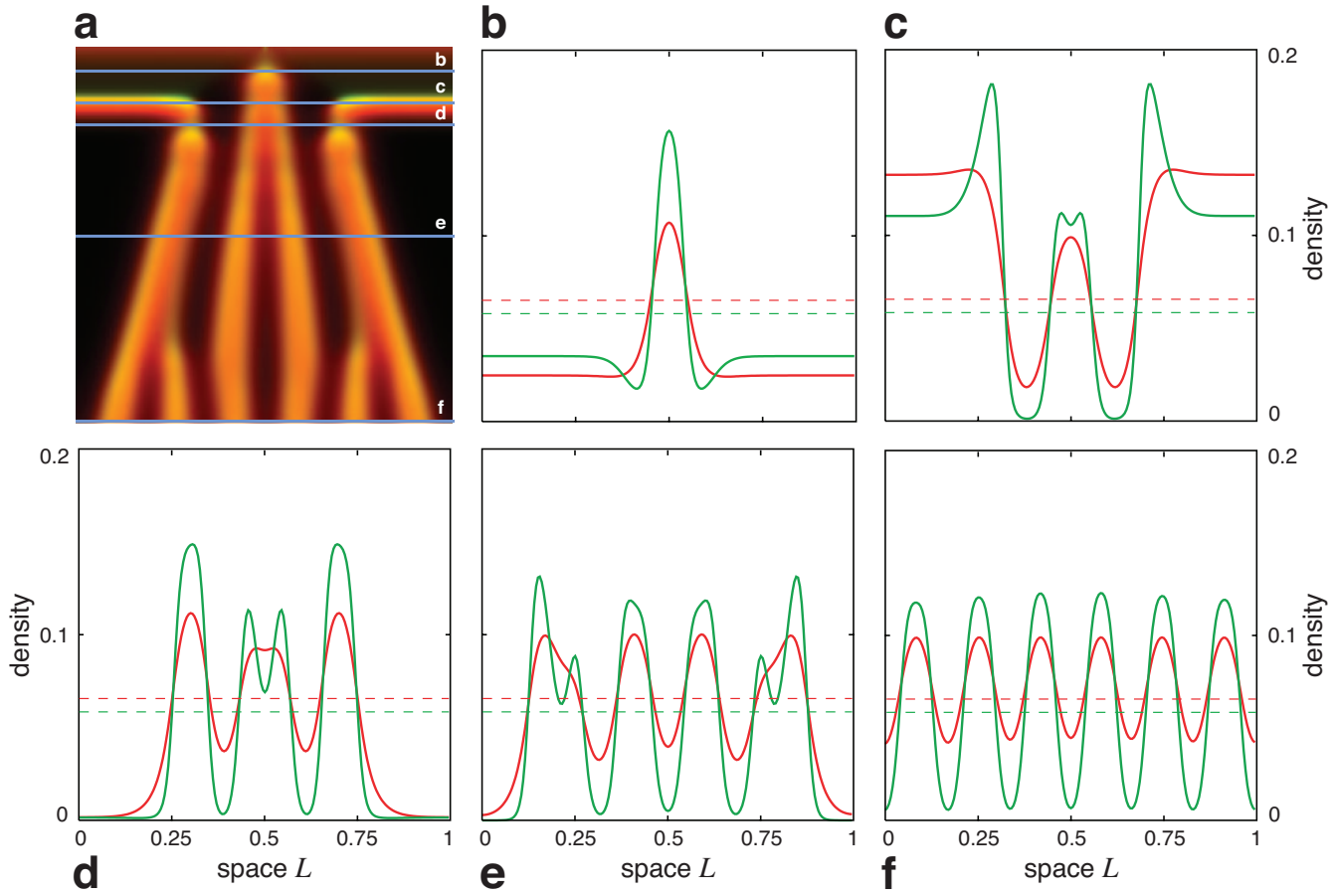

Fig. S3. Pattern formation process in ecological public goods games through diffusion-induced coexistence in 1-dimensional spatial systems. As in Fig. S2, the initial strategy distribution is homogeneous with densities near the unstable equilibrium **Q** and a perturbance in the center (increase of the cooperator density by 0.1). (*a*) Space–time plot of the pattern formation process where the ordinate denotes spatial extension and the abscissa the time (from top to bottom). The brightness of the colors indicates the density of cooperators (green) and defectors (red), both (yellow), or none (black). The horizontal lines in *a*, labeled b–f, indicate the times of the cross-sections of cooperator (green) and defector (red) densities $t = 30$ (*b*), $t = 60$ (*c*), $t = 99$ (*d*), $t = 300$ (*e*), and $t = 597$ (*f*). In *b*-*f*, the dashed horizontal lines indicate the frequencies of cooperators, $\hat{u}$, and defectors, $\hat{v}$ at the unstable **Q**. The game parameters are $N = 8$, $b = 1$, $d = 1.2$, $r = 2.3$, which yields $\hat{u} = 0.058$, $\hat{v} = 0.066$. Diffusion coefficients are $D_C = 1$ and $D_D = 10$, spatial extension is $L = 200$ and numerical integration uses $dx = 1$ and time increments of $dt = 0.1$.

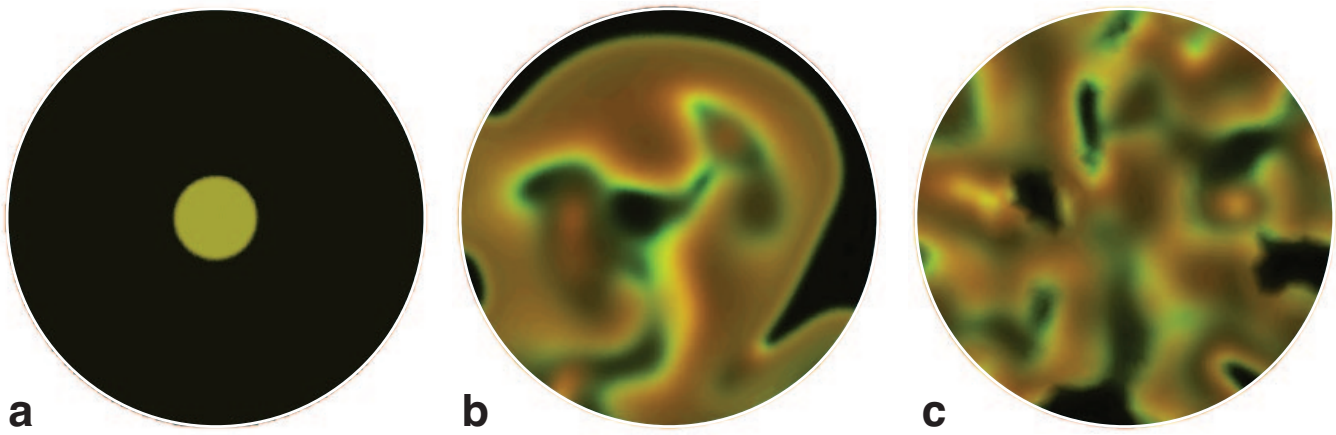

Fig. S4. Chaotic pattern formation in spatial ecological public goods. The setup is identical to Fig. 1 in the main text with the only differences that the spatial domain is circular instead of rectangular and the numerical integration of Eq. **S1** is based on the finite element method FreeFEM++ [Hecht F, Pironneau O, Le Hyaric A, Ohtsuka K (2007) Freefem++: Finite element method to solve partial differential equations. www.freefem.org]. The qualitative features of the emerging spatial patterns remain unchanged. (*a*) Initial configuration. (*b*) Snapshot at time $t = 2{,}000$. (*c*) Snapshot at $t = 7{,}000$. The parameters of the ecological public goods are $N = 8$, $d = 1.2$, $b = 1$, $r = 2.34$, $D_C = 1$, $D_D = 2$, and the initial configuration is a vacant disk with radius $R = 200$ (no flux boundary conditions) and a disk with radius $R/10$ in the center, where cooperators (green) and defectors (red) coexist at equal densities ($u_{disk} = v_{disk} = 0.1$ and $u = v = 0$ elsewhere).

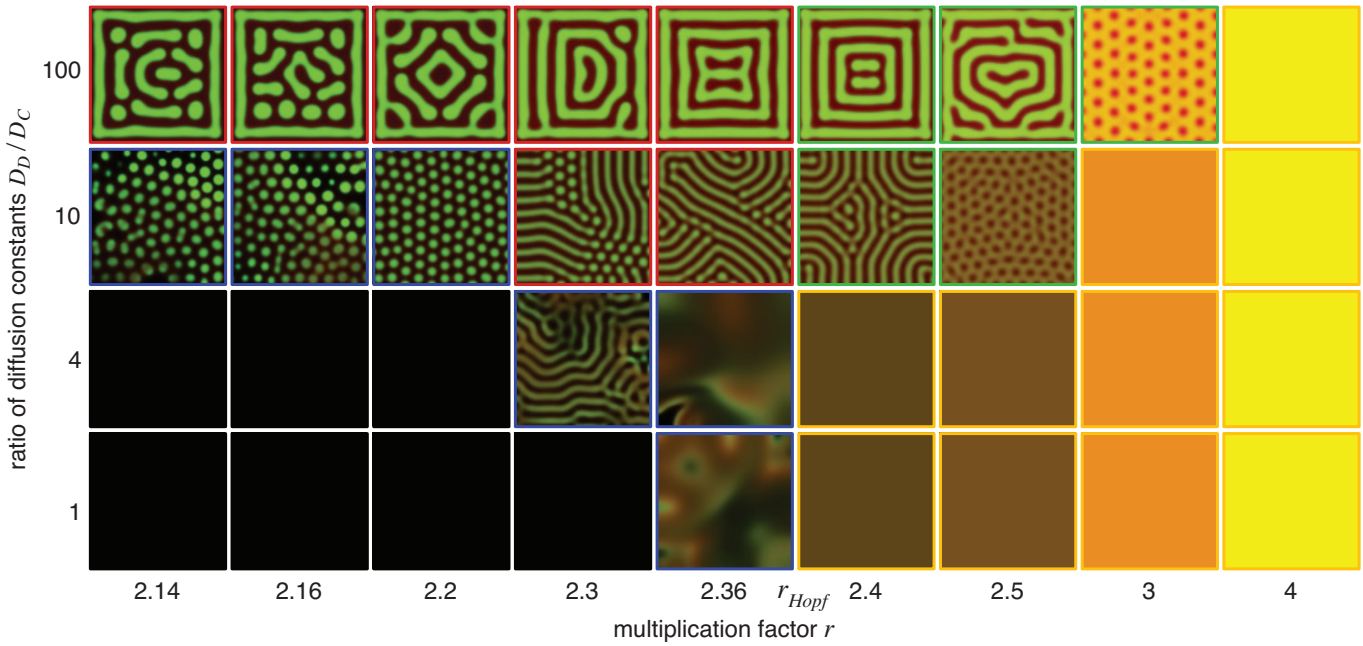

Fig. S5. Diversity of spatial distributions in terms of the ratio of the diffusion of defectors to cooperators, D_D/D_C, and the multiplication factor, r, in spatial ecological public goods games. This figure is identical to Fig. 4 in the main text with the only exception being that instead of a randomly mixed initial configuration, the initial state is given by a vacant $L \times L$ square and a homogeneous disk with radius $L/10$ in the center, where cooperators and defectors coexist at equal densities ($u_{\text{disk}} = v_{\text{disk}} = 0.1$ and $u = v = 0$ elsewhere; see Fig. 1 in the main text). The symmetry of the initial configuration leads to more symmetrical static patterns for diffusion induced instability (green frame) and diffusion induced coexistence (red frame). Homogeneous coexistence (yellow frame) remains unaffected. In all cases the qualitative features of the emerging strategy distribution remain unaffected by the initial configuration. Only the boundaries (but not the patterns) of the chaotic region (blue frame) are slightly shifted, but this is not surprising because chaotic dynamics is highly susceptible to perturbations. The parameters are $N = 8$, $d = 1.2$, $b = 1$, $D_u = 1$, $L = 283$, $dx = 1.4$, $dt = 0.1$, $r_{\text{Hopf}} = 2.3658$.

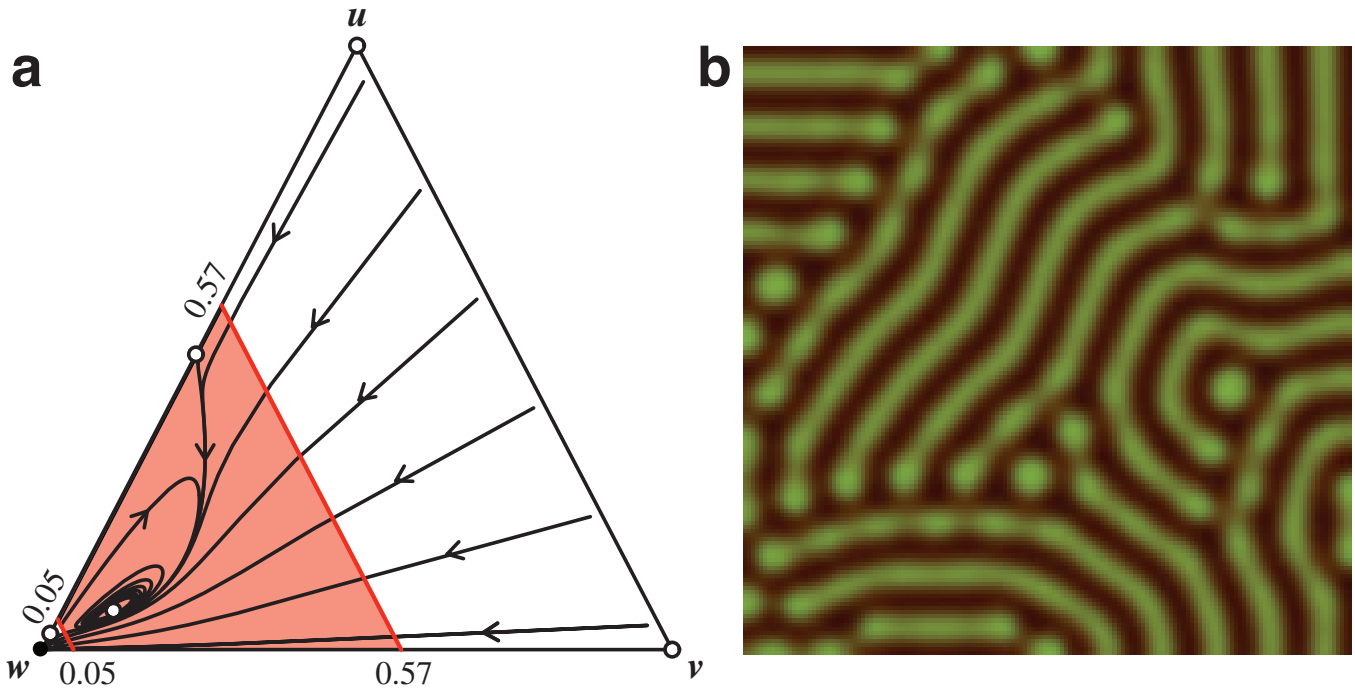

Fig. S6. Robustness of pattern formation in spatial ecological public goods games. (*a*) At or below the Hopf bifurcation, r_{Hopf}, extinction **O** is globally stable in the absence of space. (*b*) For the same parameters cooperators and defectors can coexist in a spatial setting through the spontaneous formation of heterogeneous strategy distributions. Diffusion stabilizes the unstable coexistence equilibrium **Q**. Qualitatively the same patterns emerge for different initial population densities, as indicated by the red area in *a*. Only for very low ($u + v < 0.05$) and for high ($u + v > 0.57$) population densities, coexistence is unreachable, and the population disappears just as in the absence of space. The density thresholds in *a* are numerically derived for $N = 8$, $r = 2.36$, ($r_{\text{Hopf}} = 2.3658$), $b = 1$, $d = 1.2$, $D_C = 1$, $D_D = 10$. The initial density, p, is fixed and we randomly set the cooperator density $u(x,y,0)$ according to a uniform distribution in $[0,p]$. The defector density is given by $v(x,y,0) = p - u(x,y,0)$. The time evolution for various p determines the red area.

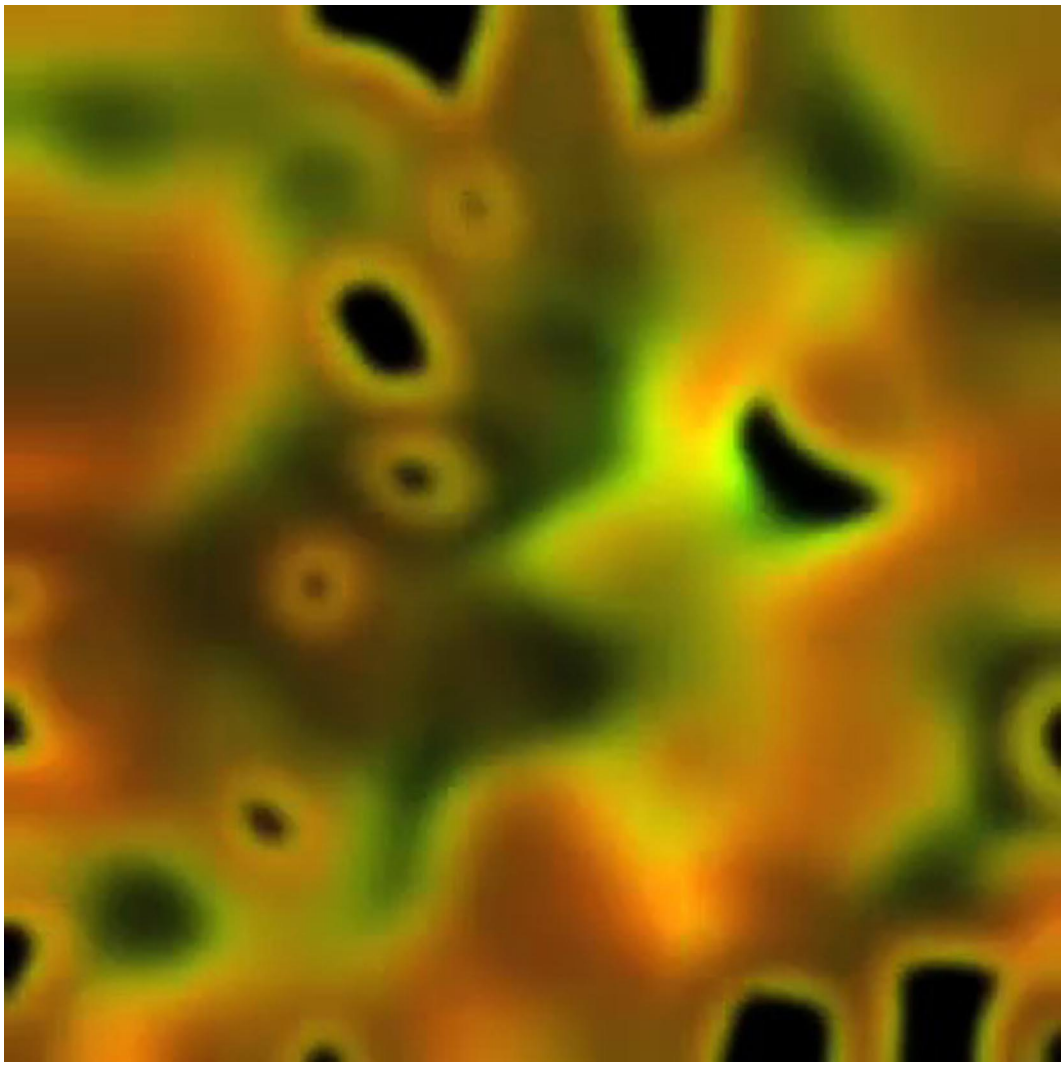

Movie S1. Spatiotemporal chaos. Onset of chaotic dynamics when starting from a symmetrical initial configuration (see Fig. 1 in main text). The deterministic dynamics should, in principle, preserve the symmetry, but it breaks down after some time because of limitations of the numerical integration combined with the exponential amplification of arbitrarily small deviations in chaotic dynamics. Parameters: $N = 8$, $r = 2.34$, $b = 1$, $d = 1.2$, $D_C = 1$, $D_D = 2$, $L = 400$, $dx = 0.8$, $dt = 0.01$ and the movie ends at time $T = 4{,}000$. The movies are highly compressed using the open standard H.264 and require QuickTime 7 or higher for playback.

Movie S1 (MOV)

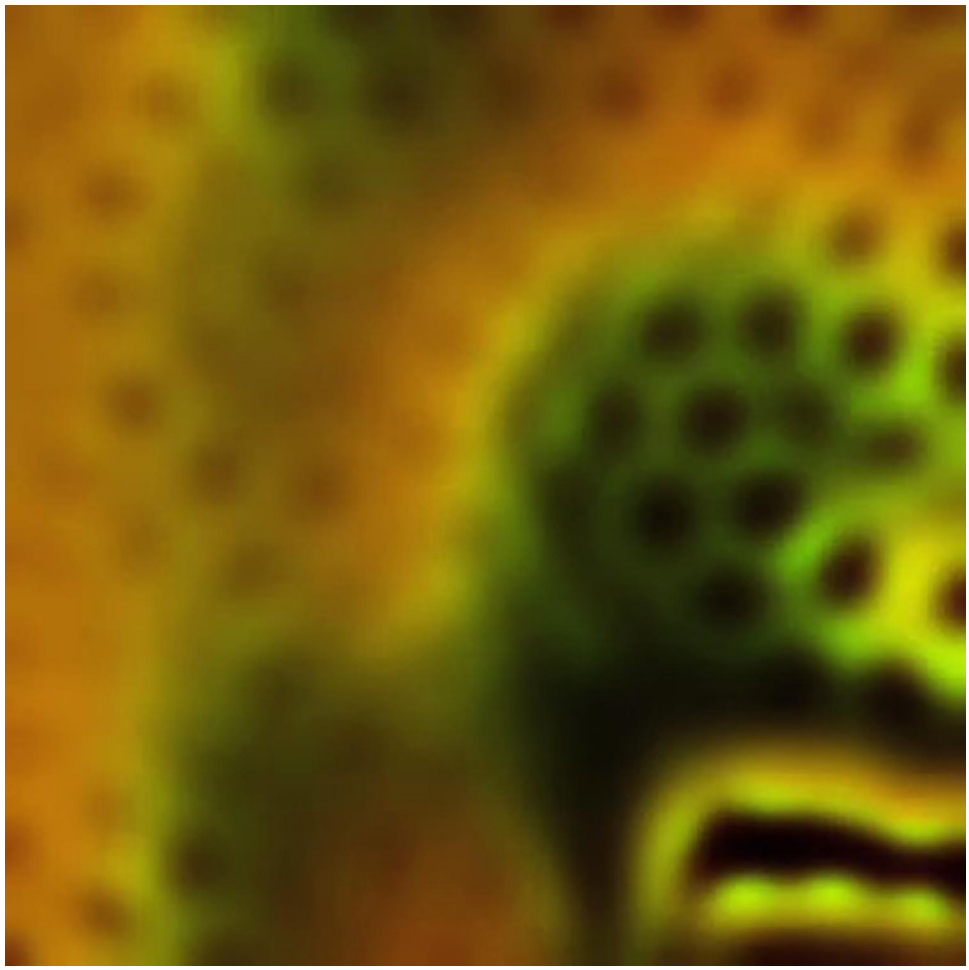

Movie S2. Intermittent activity. In the region of intermittent activity, the formation of quasistatic patterns alternates with rapid changes triggering local (or global) rearrangement and redistribution of cooperators and defectors. Parameters: $N = 8$, $r = 2.34$, $b = 1$, $d = 1.2$, $D_C = 1$, $D_D = 4$, $L = 256$, $dx = 0.8$, $dt = 0.01$ and the movie ends at time $T = 5{,}000$. The movies are highly compressed using the open standard H.264 and require QuickTime 7 or higher for playback.

Movie S2 (MOV)

Movie S3. Diffusion induced instability (Turing patterns). Cooperators and defectors form an activator–inhibitor system that destabilizes the homogeneous coexistence equilibrium **Q**. The antagonistic forces of cooperators (activators) and defectors (inhibitors) give rise to the formation of stable patterns. Parameters: $N = 8$, $r = 2.5$, $b = 1$, $d = 1.2$, $D_C = 1$, $D_D = 100$, $L = 256$, $dx = 0.8$, $dt = 0.01$ and the movie ends at time $T = 500$. The movies are highly compressed using the open standard H.264 and require QuickTime 7 or higher for playback.

Movie S3 (MOV)

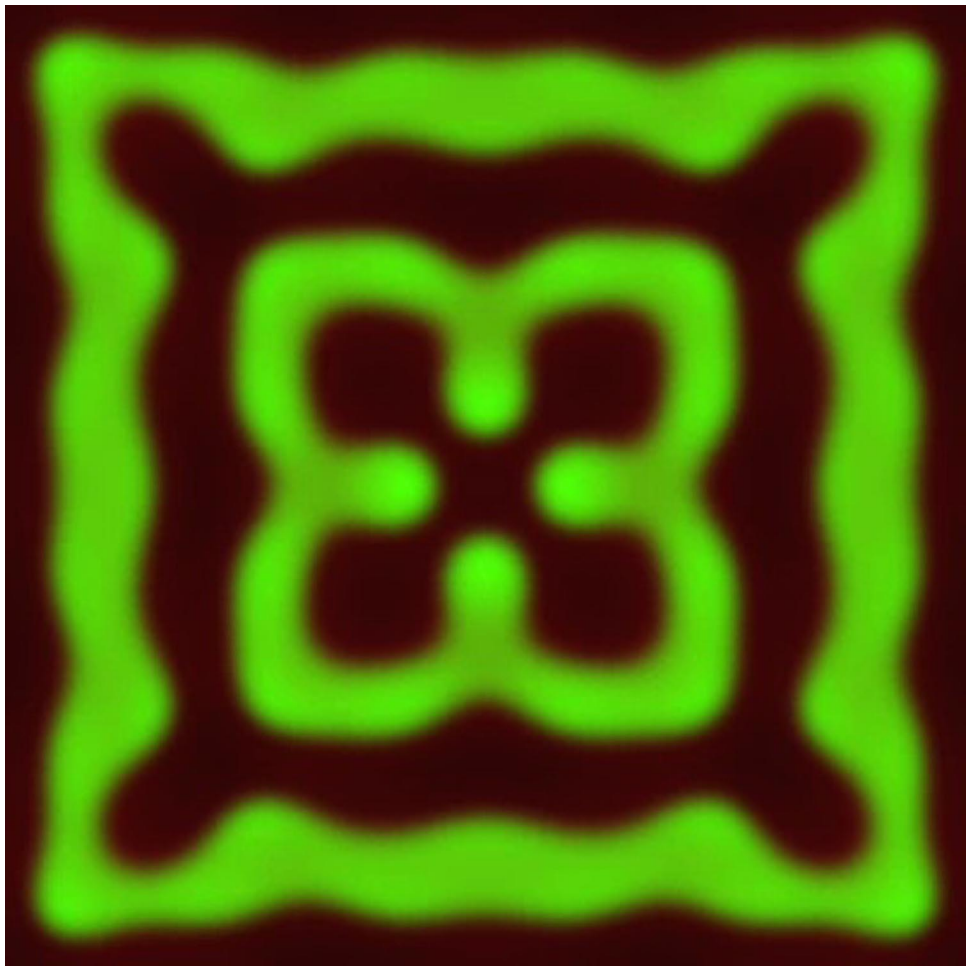

Movie S4. Diffusion induced coexistence. In the absence of space, the population goes extinct. The emerging spatial patterns are responsible for the survival of the population and permit stable coexistence of cooperators and defectors. Parameters: $N = 8$, $r = 2.2$, $b = 1$, $d = 1.2$, $D_C = 1$, $D_D = 100$, $L = 256$, $dx = 0.8$, $dt = 0.01$ and the movie ends at time $T = 2{,}000$. The movies are highly compressed using the open standard H.264 and require QuickTime 7 or higher for playback.

Movie S4 (MOV)